ACS APPLIED MATERIALS & INTERFACES

Research Article

www.acsami.org

Superhydrophilic Polyelectrolyte Brush Layers with Imparted Anti-Icing Properties: Effect of Counter ions

Sergey Chernyy,[†] Mikael Järn,[‡] Kyoko Shimizu,[§] Agne Swerin,[‡,⊥] Steen Uttrup Pedersen,[§,∥] Kim Daasbjerg,[§,∥] Lasse Makkonen,[#] Per Claesson,[‡,⊥] and Joseph Iruthayaraj*[,∥,△]

[†]Department of Micro- and Nanotechnology, Technical University of Denmark,, Produktionstorvet, 2800 Lyngby, Denmark

[‡]Chemistry, Materials and Surfaces, SP Technical Research Institute of Sweden, SE-114 86 Stockholm, Sweden

[§]Department of Chemistry, Aarhus University, Langelandsgade 140, DK-8000 Aarhus, Denmark

[∥]Interdisciplinary Nanoscience Center (iNANO), Department of Physics and Astronomy, Aarhus University, Ny Munkegade 120, DK-8000 Aarhus C, Denmark

[⊥]Department of Chemistry, Surface and Corrosion Science, KTH Royal Institute of Technology, SE-100 44 Stockholm, Sweden

[#]VTT Technical Research Centre of Finland, 02044 VTT, Finland

[△]Biological and Chemical Engineering Division, Aarhus University, Hangøvej 2, 8200 N Aarhus, Denmark

Supporting Information

ABSTRACT: This work demonstrates the feasibility of superhydrophilic polyelectrolyte brush coatings for anti-icing applications. Five different types of ionic and nonionic polymer brush coatings of 25−100 nm thickness were formed on glass substrates using silane chemistry for surface premodification followed by polymerization via the SI-ATRP route. The cationic [2-(methacryloyloxy)ethyl]-trimethylammonium chloride] and the anionic [poly(3-sulfopropyl methacrylate), poly(sodium methacrylate)] polyelectrolyte brushes were further exchanged with H^+, Li^+, Na^+, K^+, Ag^+, Ca^{2+}, La^{3+}, $C_{16}N^+$, F^-, Cl^-, BF_4^-, SO_4^{2-}, and $C_{12}SO_3^-$ ions. By consecutive measurements of the strength of ice adhesion toward ion-incorporated polymer brushes on glass it was found that Li^+ ions reduce ice adhesion by 40% at −18 °C and 70% at −10 °C. Ag^+ ions reduce ice adhesion by 80% at −10 °C relative to unmodified glass. In general, superhydrophilic polyelectrolyte brushes exhibit better anti-icing property at −10 °C compared to partially hydrophobic brushes such as poly(methyl methacrylate) and surfactant exchanged polyelectrolyte brushes. The data are interpreted using the concept of a quasi liquid layer (QLL) that is enhanced in the presence of highly hydrated ions at the interface. It is suggested that the ability of ions to coordinate water is directly related to the efficiency of a given anti-icing coating based on the polyelectrolyte brush concept.

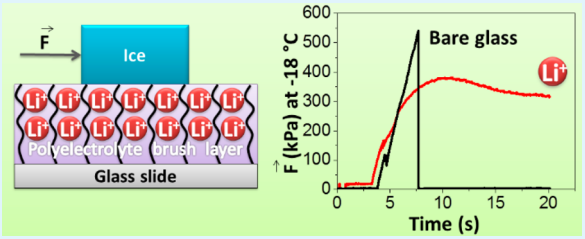

KEYWORDS: *ATRP isopropanol-water, polyelectrolyte brushes, ion exchange, anti-icing, superhydrophilic surfaces, ice adhesion*

INTRODUCTION

Ice accretion on surfaces is a critical issue in many different areas in terms of function, safety, and cost of operation. For instance, even a thin layer of ice on the wings of an aircraft may bring about severe safety risks. Accumulation of ice on the surface of wind turbine blades not only reduces the aerodynamic performance, eventually leading to decreased energy production, but may even imply a potential safety risk for people in the vicinity of the operating wind turbine. Ice accretion on heat exchanger surfaces reduces the efficiency during operation, and large amounts of energy are consumed during defrosting cycles.[1]

The main strategies to overcome icing problems are based on active anti- or deicing methods. These include electrical, thermal, and mechanical techniques to remove already accreted ice and to reduce the risk of further accretion. The main drawback with these methods is the substantial amount of energy that is required for removal of the ice. Another common strategy to remove ice or prevent ice accretion is the use of deicing fluids, which for instance are sprayed on aircrafts. However, this approach requires frequent application and the fluid might have a negative impact on the environment.[1] The ideal solution would be the use of passive methods, which rely on the chemical and physical properties of the material to prevent ice accumulation or facilitate the removal of accreted ice. In the past few years, a considerable amount of research has been made on the development of so-called icephobic materials.[2−5]

One of the common ways to characterize passive anti-icing materials is ice adhesion measurements. Numerous ways of measuring the ice adhesion on a wide range of materials have been reported, most of which involve shearing of ice from the

Received: January 3, 2014
Accepted: April 8, 2014
Published: April 8, 2014

   dx.doi.org/10.1021/am500046d | ACS Appl. Mater. Interfaces 2014, 6, 6487−6496

Scheme 1. Two-Step Solution Phase Deposition of (3-aminopropyl)trimethoxysilane (APTMS) Followed by Reaction of the Amine-Terminated Monolayer with 2-Bromo-2-methylpropanoyl Bromide (BMPB)[a]s

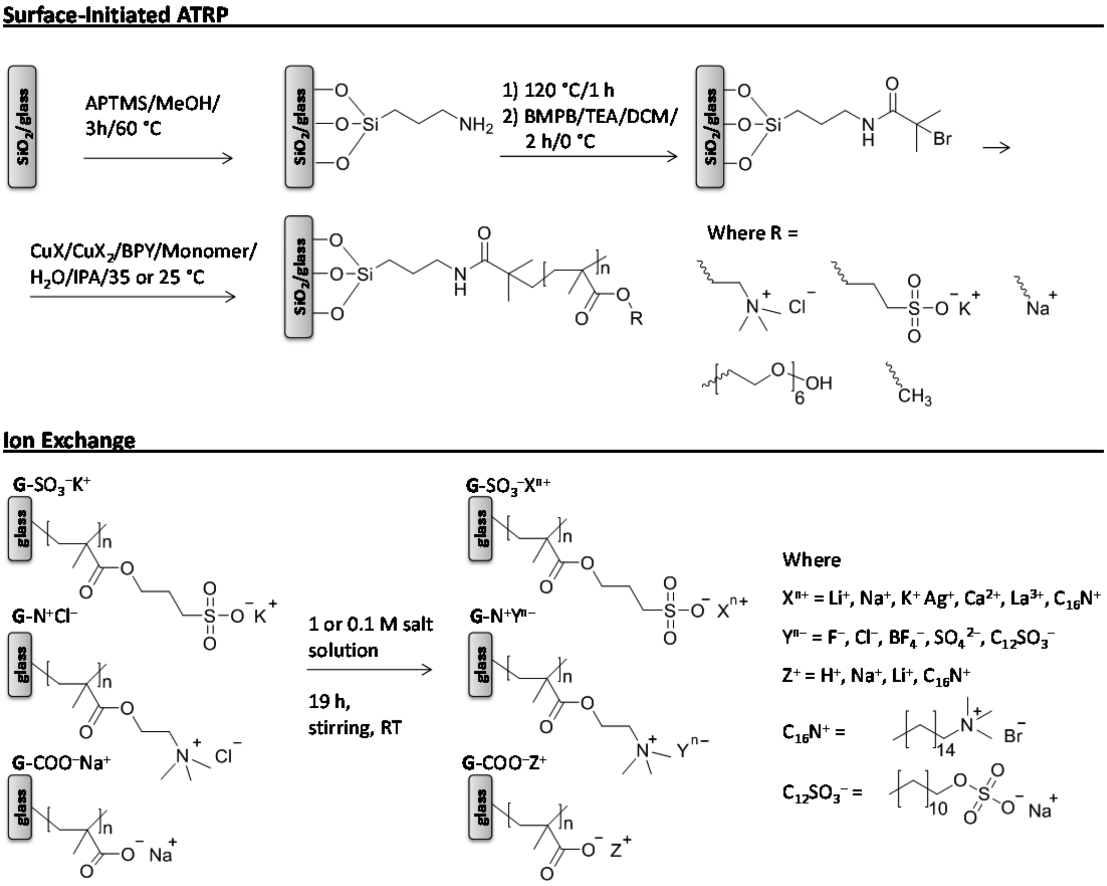

[a]Consecutively, SI-ATRP of a chosen monomer (KSPM, METAC, or monomer (KSPM, METAC, or NaMAA) was realized in the presence of catalyst, CuX and CuX_2 (X = Cl^- or Br^-), and ligand (BPY) in a 1:1 H_2O/IPA mixture. Finally, the polyelectrolyte brushes were exchanged with desired ions and used further for ice adhesion strength measurement.

surface by applying an external force.[6] A good correlation between the work of adhesion of water and ice adhesion strength has been reported by several groups.[7−12] Due to this observation, a significant effort has been devoted to superhydrophobic surfaces that exhibit high contact angles and low contact angle hysteresis. Superhydrophobic coatings have also shown promising properties as anti-icing surfaces in a number of studies,[3,13] but the efficiency of this approach has been put into doubt[6,14] and such surfaces are not necessarily the best solution. For instance, at high humidity frost formation and water condensation in the rough surface structure of superhydrophobic surfaces results in high ice adhesion strength due to the large solid-ice contact area.[15] Further, Kulinich et al. found that repeated icing/deicing cycles on superhydrophobic surfaces resulted in an increased ice adhesion strength with time, because of wear of the micro/nanostructure of the superhydrophobic surface.[16]

Another recent approach for prevention of ice accretion, conceptually different from the superhydrophobic effect, is to use a porous substrate to lock a lubricating liquid in place. Such liquidlike layers have shown promising properties as anti-ice materials.[4,17] In a recent work, Chen et al. have demonstrated the applicability of structured microporous superhydrophilic surfaces for anti-icing applications.[18]

Still another approach as reported by Murase et al.[19,20] demonstrates very low ice adhesion strength on an organopolysiloxane material containing Li^+ ions. They ascribed this result to the presence of both bound and restrained water molecules due to the hydrogen bond breaking properties of the Li^+ ions. Nevertheless, it remains unclear to what extent the ions embedded in polysiloxane matrix could have contributed to anti-icing properties.

Therefore, to further explore this concept and to increase the understanding on how different counterions affect the measured ice adhesion strength, we have prepared various surface grafted polyelectrolyte brushes in a controlled manner using surface initiated atom transfer radical polymerization (SI-ATRP). To the best of our knowledge, it is the first time that such well-defined superhydrophilic polyelectrolyte brushes have been analyzed to study the effects of counterions on ice repelling properties. Ice adhesion to hydrophilic substrates has previously only been tested on bare surfaces with inherent hydrophilic character (stainless steel, silica).[21,22] In the present work, the effects of ion incorporation in polyelectrolyte brush layers on ice adhesion strength have been examined systematically using well-defined surface chemistry.

MATERIALS AND METHODS

All chemicals were purchased from Sigma-Aldrich unless otherwise stated. Dichloromethane (DCM, ≥99.8%), methanol (99.9%), ethanol (99.9%), isopropanol (IPA, 99.8%), water (Milli-Q, 18 MΩ cm) were used as solvents.

Table 1. SI-ATRP Conditions Employed for Various Monomers and Dry Film Thickness (d) of Various Polymer Brush Layers on Si-Br Substrates[a]

substrates	monomer (M)	T (°C)	t (h)	CuX (mM)	CuX_2 (mM)	BPY (mM)	solvent IPA/H_2O	d (nm)
G-SO_3^- K^+/Si-SO_3^- K^{+b}	KSPM [1.5]	35	4	60	26	215	1/1	25 ± 2
G-N^+Cl^-/Si-N^+Cl^{-b}	METAC [1.7]	35	4	60	6.7	167	1.4/1	26 ± 2
G-COO^-Na^+/Si-COO^- Na^{+c}	NaMAA [3.1]	25	3	30	13	108	1/7	106 ± 5
G-PEG /Si-PEG^b	PEGMA [1.0]	50	4	30	17	140	1/1	20 ± 2
G-PMMA/Si-PMMA^{b,s}	MMA [5.0]	40	11	7.5	1.8	8.9	acetone	30.5 ± 1

[a]The numbers inside the square brackets represent the molar concentration of monomers. CuX, CuX_2, and BPY represent catalyst, deactivator, and the ligand, respectively. The solvent is isopropanol (IPA) unless otherwise stated. [b]CuCl/$CuCl_2$ was used, [c]CuBr/$CuBr_2$ was used. [s]Polymerization conducted in acetone.[30]

The cationic monomer, [2-(methacryloyloxy)ethyl]-trimethylammonium chloride (METAC), 80 wt % in water), was passed through inhibitor removal column (306312 Aldrich) and collected under ice cold conditions. The weakly dissociative anionic monomer, sodium methacrylate (NaMA) was synthesized by neutralization of methacrylic acid (MAA) with sodium hydroxide. The strongly dissociative anionic monomer, 3-sulfopropyl methacrylate potassium salt (KSPM, 98%) and the nonionic macro monomer, poly(ethylene glycol) methacrylate (PEGMA, M_n = 360 g mol^{-1}) were used as received.

Other chemicals used in this work, (3-aminopropyl)-trimethoxysilane (APTMS, 97%), 2-bromo-2-methylpropanoyl bromide (BMPB, 98%), CuCl (99.9%), $CuCl_2$ (99.999%), 2,2′-bipyridyl (BPY, ≥99%), LiCl (99%), lithium acetate dihydrate (99%), NaCl (99.5%), $AgNO_3$ (99%), $CaCl_2{\cdot}2H_2O$ (99.5%), $LaCl_3{\cdot}7H_2O$ (98%), NaF (99%), $NaBF_4$ (≥98%), Na_2SO_4 (99%), *N*-hexadecyl-*N,N,N*-trimethylammonium bromide ($C_{16}H_{34}N^+(CH_3)_3Br$, 99%), sodium dodecyl sulfate ($C_{12}H_{26}OSO_3^-$ Na^+, ≥99%), were used as received. Triethylamine (TEA, 99%) was kept under 4 Å molecular sieves before use to remove residual water.

Substrates. Microscope glass slides (G) (deltalab, Spain 2.6 cm × 7.6 cm) were cut into 2 cm × 5 cm pieces. Silicon (100, Silicon Valley Microelectronics) wafers with 20 nm of thermally grown oxide (**Si**) were cut into 1 cm × 1 cm pieces and used as reference surfaces for dry film thickness determination using ellipsometry. Prior to silanization the substrates were sonicated in water and ethanol followed by cleaning with piranha solution comprising of 1:3 (v/v) 30% H_2O_2: (95%) H_2SO_4 at 80 °C for 30 min. Subsequently, the plates were rinsed several times in Milli-Q water and ethanol.

Formation of Surface-Grafted ATRP Initiator Layer. Freshly cleaned glass slides and Si wafers were immersed in a solution of APTMS in methanol (20 mM) for 3 h at 60 °C without stirring, followed by rinsing in methanol and heat annealing under argon for 1 h at 120 °C. To incorporate the ATRP initiator, the APTMS modified silicon and glass substrates were reacted in a DCM solution containing BMPB (0.25 M) and TEA (0.25 M) at 0 °C for 2 h (Scheme 1) under mechanical agitation followed by thorough rinsing with DCM. The initiator modified glass and Si wafers are henceforth represented as G-Br and Si-Br, respectively.

Synthesis of Polyelectrolyte Brushes. In a typical synthesis of the strongly dissociative anionic polyelectrolyte brush, 50 g of KSPM monomer (1.5 M) and 4.462 g of BPY ligand (0.215 M) was added to 100 mL of a Milli-Q water/IPA mixture (1/1, v/v) followed by argon purging for 20 min. The catalyst mixture, composed of 0.790 g of CuCl (60 mM) and 0.465 g $CuCl_2$ (26 mM), was added under argon flow. The mixture was stirred for 15 min resulting in the formation of homogeneous dark brown solution. The initiator modified substrates, G-Br and Si-Br, were immersed into the ATRP medium and the polymerization was conducted at 35 °C with constant stirring. After 4 h of polymerization the surfaces were removed and rinsed thoroughly with water, ethanol, and dried under argon. The strong anionic polyelectrolyte brushes, poly(3-sulfopropyl methacrylate), on glass and silicon are represented as G-$SO_3^-K^+$ and Si-$SO_3^-K^+$ respectively. A similar procedure was adopted to synthesize the weak anionic polyelectrolyte, poly(sodium methacrylate), represented as (G-COO^-Na^+, Si-COO^-Na^+) and the strong cationic polyelectrolyte brushes, poly(2-(methacryloyloxy)ethyl]trimethylammonium chloride), represented as (G-N^+Cl^-, Si-N^+Cl^-). The SI-ATRP conditions used for the synthesis of the various polyelectrolyte brushes are provided in Table 1. The deactivator concentration was three times lower for ATRP of METAC (10%) compared to KSPM (30%) to compensate for the presence of chloride counterions in the structure of the former monomer. Excess chloride ions during ATRP will suppress dissociation of the deactivator complex $CuCl(BPY)_2$ and increase the effective concentration of the deactivator species, which would result in diminished rate of brush growth.[23] In spite of the fact that 30% of deactivator and 10 °C lower temperature was used for the synthesis of poly(sodium methacrylate) brushes, the maximum thickness of poly(sodium methacrylate) is 4 times larger compared to other ionic brushes, which is in agreement with the results of Tugulu et al.[24]

Synthesis of PEGMA Brushes. One hundred sixteen grams of PEGMA macromonomer (1.02 M), 0.93 g of $CuCl_2{\cdot}2H_2O$ (0.017 M), and 7.1 g of BPY ligand (0.14 M) was added to 315 mL of a 1/1 IPA/Milli-Q water mixture. The mixture was stirred under argon atmosphere until a homogeneous blue color solution is obtained. After another 10 min of argon purging, 1.25 g of CuCl (0.03 M) was added and the solution was purged continuously with argon. The solution mixture was stirred at 50 °C for another 10 min and transferred under argon atmosphere to the polymerization chamber containing initiator modified substrates kept at 50 °C. After 4 h of polymerization, the substrates were removed and rinsed thoroughly with Milli-Q water and stored under water overnight with stirring. The surfaces were subsequently rinsed with ethanol and dried under argon. The PEG brush substrates are denoted as G-PEG, Si-PEG.

Ion Exchange. The counterion exchange of the polyelectrolyte brushes were carried out by immersing the brushes into a solution of appropriate salt concentration at constant stirring for 19 h. For the exchange of monovalent ions 1 M concentration of salt was used, while for divalent and trivalent ions 0.1 M solutions were utilized. After the ion exchange the plates were rinsed 3 times with Milli-Q water and ethanol and argon dried. Ion exchange of strong polyelectrolyte brushes G-$SO_3^-K^+$, G-N^+Cl^- were conducted in pH neutral salt solutions and in the case of the weak polyelectrolyte brush, G-COO^-Na^+, ion exchange was carried out in slightly alkaline solutions.

Similarly, the counterions of polyelectrolyte brushes were exchanged for surfactants using 0.01 M ionic surfactant solutions, which in terms of critical micelle concentration (CMC) corresponds to C/CMC = 1.25 for the anionic surfactant, sodium dodecyl sulfate (SDS, $C_{12}H_{26}OSO_3^-Na^+$) and C/CMC = 11.1 for the cationic surfactant, cetyltrimethylammonium bromide (CTAB, $C_{16}H_{34}N^+(CH_3)_3Br$) (Scheme 1). After the surfactant treatment, the plates were rinsed with water. The surfactant exchanged polyelectrolyte brushes are represented as G-N^+DS^-, G-CTA^+.

Contact Angle Measurements. Static and dynamic contact angle measurements on polymer brushes have been performed using the tilt method and the sessile drop method (FTA Instruments, USA). The tilt method was preferred on polyelectrolyte brushes since the water droplet was able to slide off without pinning. In practice, the polyelectrolyte brush surface was inclined to 40° before the addition of Milli-Q water (1 μL in volume) and the droplet sliding was recorded using a video camera. The advancing and the receding angles were

Scheme 2. Tilt Method to Determine Advancing (θ_a) and Receding (θ_r) Contact Angles on Superhydrophilic Polyelectrolyte Brushes on Glass Substrates[a]

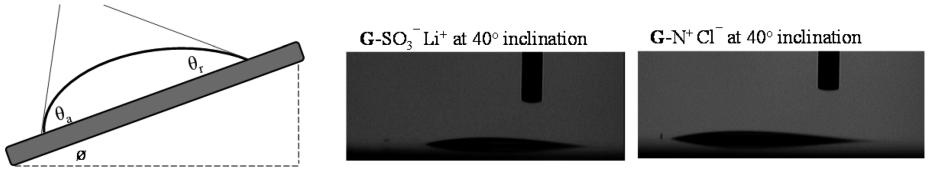

[a]The tilt angle (ø) was fixed at 40°. Pictures correspond to video frames wherein the droplet has attained equilibrium shape on G-SO_3^- Li^+, G-N^+Cl^- while sliding along the substrate at tilt angle (ø = 40°).

Scheme 3. (A) Measurement Setup for Measuring Ice Adhesion Strength on Various Hydrophilic Polymer Brushes via Application of a Shear Force in the Tangential Direction to the Ice-Containing Cuvette Resting of the Substrate Surface; (B) Set-up for Freezing Water on Polymer Brush-Modified Glass Substrates[a]

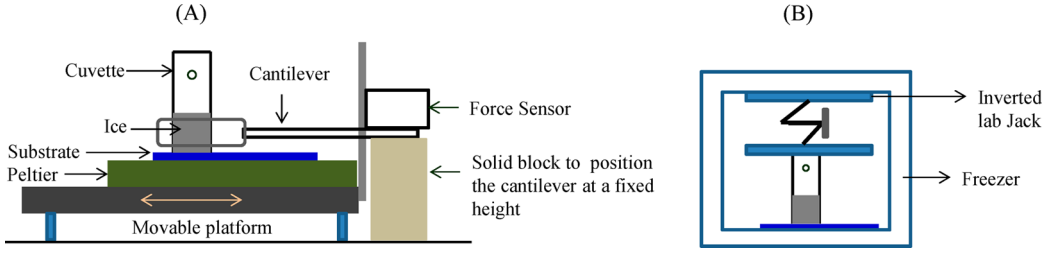

[a]A hydrophobized cuvette of 1 cm^2 cross sectional area firmly fixed on the glass substrate using an inverted lab jack and placed in the freezer kept at appropriate temperature.

measured corresponding to the frames wherein the droplet has attained the equilibrium shape. The contour of tilted drops were fitted numerically using B-spline snakes (active contours) to determine accurately the advancing and receding contact angles.[25] Scheme 2 shows the contact angle measurement profile alongside with the actual video frames corresponding to lithium ion-exchanged anionic polyelectrolyte brushes (G-SO_3^- K^+) and cationic polyelectrolyte brush with chloride counterions (G-N^+Cl^-).

Unlike polyelectrolyte brushes, water drops on partially hydrophilic (poly(methacrylic acid)) and partially hydrophobic (poly(methyl methacrylate)) polymer brushes remained pinned to the surface even though the tilt angle has been increased up to 80°. Therefore, dynamic sessile drop method was employed on these surfaces by adding/removing water using a fine needle to determine advancing and receding contact angles.

Ellipsometry, Profilometry, and XPS. Details concerning ellipsomtery, profilometry, and X-ray photoelectron spectroscopy (XPS) are presented in the Supporting Information.

Freezing and Ice Adhesion Measurements. The adhesion strength of ice on various polymer brush-ice interfaces was measured with a modified slip/peel tester (IMASS SP-2000), equipped with a force sensor and a Peltier cooling stage. Plastic cuvettes were hydrophobized by plasma treatment to avoid leakage. The cuvettes were attached to the substrate with a lab jack, thereafter they were filled with 1 mL of Milli-Q water through a hole in the cuvette. The assembly was placed on a cold metal plate inside the freezer (−18 or −10 °C) for 15 min. After freezing for 15 min the lab jack was removed and the cuvette with frozen water was left in the freezer for additional 15 min. Just prior to adhesion measurement the sample was transferred onto the Peltier element on the peel tester maintained at either −18 °C or −10 °C. The chosen freezing temperatures are relevant for industrial heat exchanger applications. The force transducer arm was placed around the cuvette (Scheme 3) and the sample was moved at a speed of 0.3 mm/s. The probe to sample distance is ca. 3 mm in this setup and the positioning of the probe has been done consistently to the specified height by using a solid block of fixed height as a stop (Scheme 3).[26] After the alignment of the sensor the block was removed just prior to measurement. The measured force (in kN) is normalized with respect to contact area (in m^2) and thus, the ice adhesion strength is expressed in kilopascal (kPa) [1 kPa = 1 kNm^{-2}].

RESULTS AND DISCUSSION

Structural Aspects of Polymer Brushes. SI-ATRP synthesis of the various monomers has been conducted on Si-Br and **G**-Br initiator layers according to the conditions delineated in Table 1. The efficacy of the polymerization process was monitored by measuring the thickness of the various polymer brush layers grown on Si-Br substrates by ellipsometry. To ensure the comparison between glass and silicon substrate to be relevant the initiator layers and the polymerization on G-Br and Si-Br has been conducted identically in the same reaction bath.

With the exception of the poly(sodium methacrylate) brush (Si-COO^- Na^+) the thickness values for other polymer brushes fall within 20-30 nm (Table 1). Klok et al.[24] have studied the effects of monomer concentration, pH and temperature on the thickness of poly(sodium methacrylate) brushes obtained via copper mediated surface initiated polymerization of sodium methacrylate (NaMA) monomer in water. The most extraordinary behavior of NaMA monomer is noticeable in the temperature effects. In contrast to many other methacrylate monomers the rate of polymerization of NaMA is significantly higher at room temperatures resulting in very thick brushes compared to the very thin layers obtained at high temperatures. The other factors such as the disproportionation of copper(I) complexes in water, aqueous speciation of copper complexes at different pH and the coordination of NaMA monomer to copper complex has not been well understood in the context of surface initiated copper mediated polymerization of NaMA.

To gain some control on the thickness of poly(sodium methacrylate) brushes we chose to vary the dielectric constant of the solvent system based on the previous study,[27] which shows that the addition of a low dielectric constant solvent to water significantly reduces the disproportionation of Cu(I)

dx.doi.org/10.1021/am500046d | ACS Appl. Mater. Interfaces 2014, 6, 6487−6496

Table 2. Elemental Composition of Various Polyelectrolyte Brushes in Atomic Percent (at %) Determined from XPS Survey Spectra.[a]

polymer brush	C	O	Si	S	major ion	Σion/S	C/S
G-SO_3^- K^+[b]	43.9	36.9	5.6	4.9	3.1 (K^+)	1.5	9.0
G-SO_3^- Li^+[c]	52.1	35.8	2.0	6.4	3.7 (Li^+)	0.6	8.1
G-SO_3^- Na^+	49.3	35.0	1.9	5.8	8.1 (Na^+)	1.4	8.6
G-$SO_3^-$$Ag^+$[d]	41.1	40.9	6.9	4.6	6.3 (Ag^+)	1.5	9.0
G-SO_3^- Ca^{2+}	51.0	36.3	3.6	6.0	3.3 (Ca^{2+})	1.1	8.4
G-$SO_3^-$$La^{3+}$[e]	33.3	40.7	19.6	3.4	2.4 (La^{3+})	2.4	9.9
G-$SO_3^-$$CTA^+$	80.3	13.7	0	2.8	3.3 ($C_{16}N^+$)	1.2	29.1
polymer brush	C	O	Si	N^+	major ion	Σion/N	C/N
G-N^+Cl^-	71.8	15.1	0	7.9	5.2 (Cl^-)	0.7	9.0
G-N^+F^-[f]	19.9	54.1	19.8	2.3	1.0 (F^-)	0.4	8.7
G-$N^+BF_4^-$	49.1	23.1	6.4	5.7	3.3 (BF_4^-)	0.6	8.7
G-$N^+SO_4^{2-}$	65.5	24.3	0	7.1	2.9 (SO_4^{2-})	0.8	9.2
G-N^+DS^-	74.1	19.0	0	3.8	3.2 ($C_{12}SO_3^-$)	0.8	19.7
polymer brush	C	O	Si		major ion	Σion/O	C/O
G-COO^- H^+[g]	69.7	29.7	0		0	0.01	2.3
G-COO^- Na^+[h]	63.6	26.1	0		9.5 (Na^+)	0.7	2.4
G-COO^- Li^+	63.3	28.0	0		8.7 (Li^+)	0.6	2.3
G-COO^- CTA^+	88.0	8.3	0		3.5 ($C_{16}N^+$)	0.8	10.7
polymer brush	C	O	Si		major ion	ion/O	C/O
G-PMMA	73.8	25.7	0.4				2.8
G-PEG	60.0	33.7	5.8				1.8

[a]Photoelectrons used for atomic percent calculations: C 1s, O 1s, N 1s, Na 1s, Li 1s, B 1s, F 1s, K 2s, Si 2p, S 2p, Cl 2p, Ca 2p, Cu 2p, Ag 3d, and La 3d. Additional elements detected (in At.%). [b]N (1.3), Na^+ (3.4), Ca^{2+} (0.5), Cu^{2+} (0.5). [c]Na^+ (0.1). [d]Na^+ (0.3). [e]Ca^{2+} (0.4).[f]Ca^{2+} (1.5), Na^+ (0.7), Mg^{2+} (0.5). [g]Na^+ (0.7). [h]Cu^{2+}(0.8).

complex. Among other solvent systems tested the isopropanol-water mixture provided a better stability of ATRP medium and a reproducible thickness of the hydrophilic brushes. The average thickness values reported in Table 1 for various polymer brushes correspond to measurements performed on three independent silicon plates. The high thickness obtained in the case of Si-COO^- Na^+ is due to high water content (88% H_2O and 12% IPA) of the reaction medium. Previous works done by different research groups show that SI-ATRP of hydrophilic monomers conducted in aqueous homogeneous media proceeds fast and yields remarkably thick polymer films on the order of several hundreds of nanometers.[24,28,29]

Ion Exchange in Polyelectrolyte Brush Layers. The counterion exchange of as-synthesized polyelectrolyte brush layers was accomplished by immersion of the modified substrate in the appropriate salt solution as described in the experimental section. The elemental composition of the various polyelectrolyte brush layers as determined from XPS measurements are reported in Table 2. (see also the Supporting Information, SI1). Several characteristic features of the polyelectrolyte brush layers can be deduced from Table 2. First we observe that the K^+ counterions of G-SO_3^- K^+, has been completely exchanged for Li^+, Na^+, Ag^+, Ca^{2+}, and La^{3+} indicating efficient ion exchange of G-SO_3^- K^+ polyelectrolyte brush layers.

The XPS spectra of the anionic polyelectrolyte brush layer (G-SO_3^- K^+) include a weak Si signal originating from the underlying initiator and/or glass substrate, whereas no Si signal was observed in the case of the cationic polyelectrolyte brush (G-N^+Cl^-). Furthermore, the observed C/S ratio (= 9) of the G-SO_3^- K^+ brush is higher than the expected value (= 7) because the uninitiated groups at the glass substrate also contributes to the total carbon content. In contrast the observed C/N ratio (= 9) of G-N^+Cl^- brush is consistent with the expected value (= 9). These observations suggest that the cationic polyelectrolyte brush is denser than the anionic polyelectrolyte brush.

The exchange of K^+ ions for the bulky surfactant cation, $C_{16}N^+$ (G-$SO_3^-CTA^+$) has resulted in the complete disappearance of Si signal indicating that the surfactant adsorption has resulted in a densely mixed polyelectrolyte−surfactant film.[31−33]

The charge balance in the polyelectrolyte brush layer is expressed as charge normalized ion/S ratio and hence for a fully charge balanced sulfonate group the ion/S ratio is expected to be unity.[34] Table 2 shows that the ion/S ratio deviates from unity (0.6 to 1.5 for different counterions with one low value at 0.4 and high at 2.4) and such deviations are not due to physical trapping of the excessive salt solution inside the collapsed films since the corresponding salt counterions (e.g., Cl^- in LiCl and $LaCl_3$ salts) are not detected. One plausible source of error could originate because of the dependence of inelastic mean free path of photoelectrons in the layer on the kinetic energy of the emitted photoelectrons. This is not considered when surface data is reported as atomic %.

Anion exchange has also been observed within **G**-N^+Cl^- brushes (Table 2). Chloride ions have successfully been replaced with F^-, BF_4^-, SO_4^{2-}, and DS^- ions. We note that the conditioning of G-N^+Cl^- in F^- and BF_4^- solutions resulted in decreased carbon content of the polyelectrolyte brush as inferred from the increase in silicon and oxygen signal of G-N^+F^- and G-$N^+BF_4^-$. This is ascribed to the partial removal of the polyelectrolyte brush through fluoride triggered Si−O bond cleavage at the brush -substrate interface.[35] Nevertheless, the C/N ratio of G-N^+F^- and G-$N^+BF_4^-$ is similar to other ion exchanged films indicating that the ionizable monomeric groups were not degraded upon exchange with fluoride-containing anions.

In the case of G-COO^- Na^+ brushes the ratio of Na^+/COO^- is less than unity ($2 \times Na^+/O = 0.8$ at %). That is presumably due to partial conversion of G-COO^- Na^+ to G-COO^- H^+ via protonation of the carboxylate group during the water washing step.[24,36] Estimated from XPS the amount of protonated groups was found to be 35%. Further conditioning at pH 4.5 for 1h protonates all carboxylates and expels sodium ions from the brush layers (Table 2).

Wetting Properties. The polymer brushes employed in this work can be classified into three categories based on their wetting characteristics as presented in Table 3. All polyelectrolyte brush series (G-$SO_3^-X^{n+}$, G-N^+Y^{n-}, and G-COO^-Z^+) excluding surfactant treated ones are classified as superhydrophilic because they all satisfy at least two of the following criteria: low static contact angle ($\theta < 10°$), low hysteresis ($H < 10°$), and contact line velocity of minimum 1 mm s^{-1} at 40° tilt angle. Both G-COO^-H^+ and G-PEG exhibit relatively high static contact angle and contact angle hysteresis ($25° < \theta < 45°$, $20° < H < 30°$) and they are henceforth classified as partly hydrophilic. Despite the high hysteresis, water droplets on the G-PEG surface slides off slowly (0.2 mm s^{-1}) at 40° tilt.

Table 3. Wetting Properties of Various Polymer Brush Layers: Static Contact Angle (θ_s), Advancing Contact Angle (θ_a), Receding Contact Angle (θ_r), Contact Angle Hysteresis (H), and Velocity of Contact Line (v) Measured at 40° Tilt Angle[a]

polymer brush	θ_s (deg)	θ_a (deg)	θ_r (deg)	H (deg)	v (mm s^{-1})
G-SO_3^- K^+	<7	9	4	5	2.3
G-SO_3^- Li^+	7	11	5	6	4.2
G-SO_3^- Na^+	<7	10	6	5	1.6
G-$SO_3^-Ag^+$	<7	18	11	7	0.0
G-SO_3^- Ca^{2+}	<7	10	5	6	1.6
G-SO_3^- La^{3+}	10	12	7	5	0.0
G-N^+Cl^-	<7	10	5	5	1.0
G-$N^+BF_4^-$	7	25	9	16	0.0
G-$N^+SO_4^{2-}$	<7	12	5	7	0.0
G-$N^+C_{12}SO_3^-$	90	97	16	81	0.0
G-COO^- H^+	22	48	21	27	0.0
G-COO^- Na^+	12	13	7	6	1.7
G-COO^- Li^+	10	14	6	7	1.2
G-$COO^-C_{16}N^+$	78	93	18	75	0.0
G-PEG	40	87	57	30	0.2
G-PMMA	70	78	60	18	0.0

[a]The standard deviation values for all contact angle measurements ≤1.5 and for contact line velocity is 0.1 mm s^{-1}.

Furthermore, a clear delay (ca. 5 s) in the spreading behavior of the water droplet was observed for all multivalent ions and Ag^+. This is tentatively attributable to a gradual release of ionizable groups coordinated by multivalent ions in dry state upon contact with water. Silver ions also follow this trend in contrast to other monovalent ions. Because G-$SO_3^-Ag^+$ brushes have a possibility to form an extended polymeric network composed of sulfonate groups bridged by silver ions, silver-exchanged brushes exist in a "cross-linked" state similar to the state of the brushes containing multivalent ions.[37,38] When the water droplet is applied, silver sulfonate groups at the brush–water interface start to dissociate slower compared to easily ionizable Li^+, Na^+, or K^+ sulfonate groups. Hence silver-saturated polymer brushes resemble more multivalent-exchanged ones.

In general, all surfactant-exchanged polyelectrolyte brush layers are partially hydrophobic exhibiting similar contact angle values, 82, 90 and 78° for G-$SO_3^-CTA^+$, G-N^+DS^-, and G-COO^-CTA^+, respectively, and high contact angle hysteresis. The high hysteresis values ($75° \leq H \leq 81°$) is due to chemical heterogeneity originating from the stoichiometric mixture of hydrophilic (N^+, SO_3^-, COO^-) and hydrophobic ($C_{16}N^+$, $C_{12}SO_3^-$) groups on the surface. The extent of surfactant exchange into the various polyelectrolyte brushes, as assessed using surfactant/polyelectrolyte ratio obtained from XPS data (Table 2), correspond to N/S = 1.2 for G-$SO_3^-CTA^+$, S/N = 0.8 for G-N^+DS^-, and N/O = 0.8 for G-COO^-CTA^+. These values indicate nearly 1:1 exchange of counterions by surfactant molecules, which changes the surface properties from complete wetting to partial wetting with moderate hydrophobicity. It also means that there could possibly be no surfactant aggregates present within the brushes after rinsing because such aggregates would have resulted in ratios significantly greater than unity.[31,39,40]

Ice Adhesion Measurements. The ice adhesion pressure versus time profile on bare glass substrates (G) and lithiated polyelectrolyte brush layers (G-$SO_3^-Li^+$) is shown in Figure 1. On bare glass substrate the ice detachment process exhibits two different modes depending on the freezing temperature. At −18 °C, the pressure reaches a maximum value followed by a steep fall to zero. This is characteristic of a cohesive breakage in the ice, leaving a thin layer of ice on the surface. In contrast, at −10 °C and −5 °C, the initial increase in force is followed by a constant force resulting in sliding of the ice along the substrate.

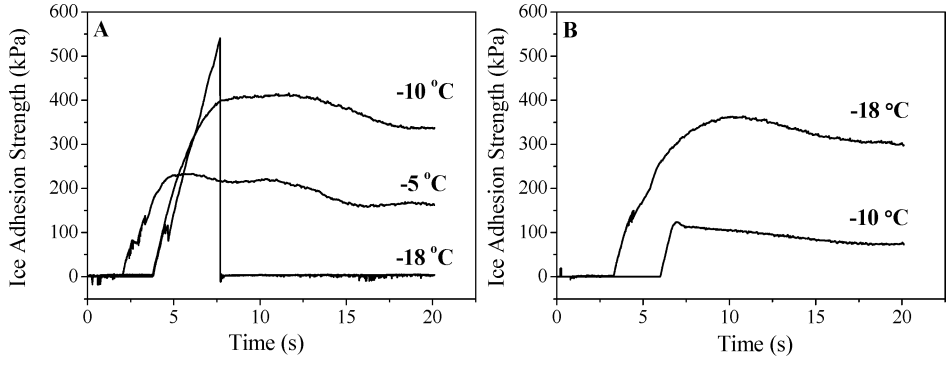

Figure 1. Ice adhesion strength versus time measured at a constant pull rate (0.3 mm s^{-1}) on (A) bare glass and (B) G-SO_3^- Li^+ substrates at different freezing temperatures.

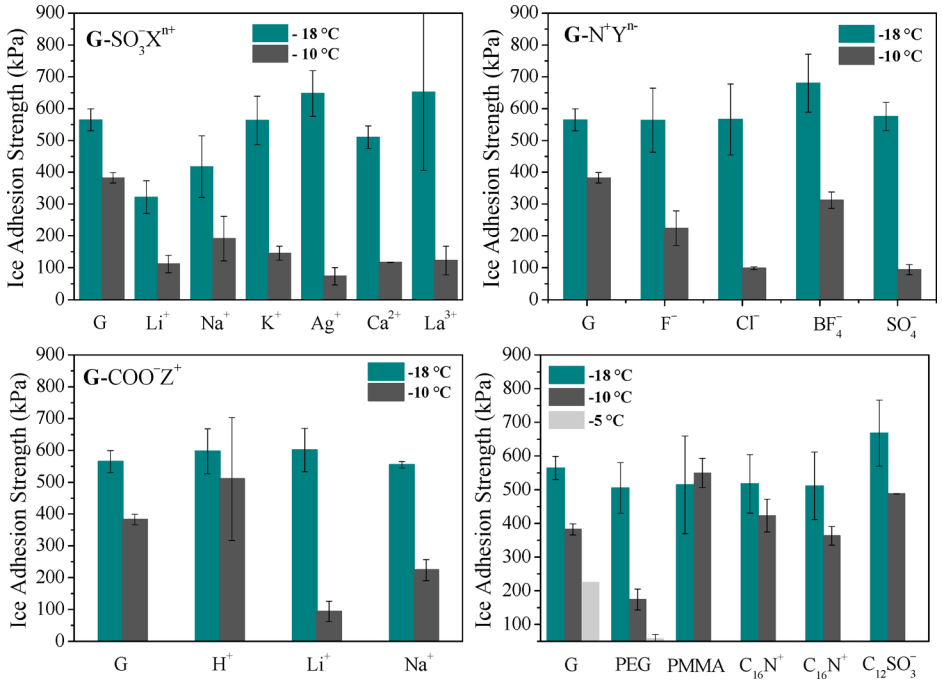

Figure 2. Ice adhesion strength measured at −18 °C and −10 °C on bare glass (G), strong anionic (G-$SO_3^-X^+$), strong cationic (G-N^+Y^{n-}), and weak anionic (G-COO^-Z^+) polyelectrolyte brush layers comprising of different types of counterions (X^{n+} = Li^+, Na^+, K^+ Ag^+, Ca^{2+}, $C_{16}N^+$, La^{3+}; Y^{n-} = F^-, Cl^-, BF_4^-, $C_{12}SO_3^-$, SO_4^{2-}; and Z^+ = H^+, Li^+, $C_{16}N^+$, Na^+). Ice adhesion strengths on G-PEG also measured at −5 °C. . The error bars correspond to standard deviation obtained on 3−5 independent substrates and correspond to 95% of the confidence interval.

Somewhat similar behavior was observed by Jellinek who reported occurrence of the adhesive breaks of ice from stainless steel substrates at temperatures down to −13 °C, whereas at lower temperature only sharp cohesive breakage was observed.[41]

The ice adhesion pressure versus time profile on lithiated polyelectrolyte brush (G-SO_3^- Li^+) display sliding of ice (Figure 1B) both at −18 °C and −10 °C. The ice adhesion strength on G-SO_3^- Li^+ is reduced by ca. 40% at −18 °C and ca. 70% at −10 °C in comparison to that measured on the bare glass substrate at the respective freezing temperatures. This is remarkable considering that the polyelectrolyte brush thickness is only a few tens of nanometer. Earlier works on anti-icing have predominantly focused on superhydrophobic coatings with thickness on the order of hundreds of nanometers to several micrometers.[10,42]

Having established the positive effects of lithium ions on reducing ice adhesion strength, we conducted a systematic investigation on the effects of various types of ions on ice adhesion strength. To this end, both anionic and cationic polyelectrolyte brushes were prepared and subsequently ion-exchanged with different types of cations and anions. Furthermore, to better understand the ion effects, we also conducted ice adhesion tests on a set of nonionic hydrophilic and hydrophobic polymer brushes such as poly(ethylene glycol methacrylate) [G-PEG], poly(methyl methacrylate) [G-PMMA], and surfactant ion-exchanged polyelectrolyte brushes (G-N^+DS^-, G-$SO_3^-CTA^+$, and G-COO^-CTA^+).

The different sets of ions were chosen on the basis of their ability to structure water molecules in isotropic dilute aqueous solution. Some of these ions (e.g., Li^+, Ca^{2+}, La^{3+}) are known as kosmotropes, or structure making ions, and have a tendency to disrupt water hydrogen bonds because of their high charge density, whereas low charge density ions (K^+, Cl^-, BF_4^-) do not coordinate water dipoles strongly and are called chaotropes or structure breaking ions.[43,44] The ice adhesion strengths measured at different freezing temperatures on polymer brush layers containing various ions are summarized in Figure 2.

Figure 2 shows that at −18 °C the maximum reduction in ice adhesion strength (25−40%) is exhibited by polyelectrolyte brushes (G-$SO_3^-Li^+$, G-$SO_3^-Na^+$) consisting of kosmotropic counterions, the ions that are strongly hydrated as characterized by negative water structural entropy ($\Delta S_{struc,Li}^+$ = −52 J K^{-1} mol^{-1}, $\Delta S_{struc,Na}^+$ = −14 J K^{-1} at 25 °C).[43] On the other hand, the polyelectrolyte brushes consisting of chaotropic counterions (G-SO_3^- K^+, G-N^+Cl^-, and G-$N^+SO_4^{2-}$), the ions that are less hydrated as characterized by their positive water structural entropy ($\Delta S_{struc,K}^+$ = +47 J K^{-1} mol^{-1}, $\Delta S_{struc,Cl}^-$ = +58 J K^{-1} and $\Delta S_{struc,SO4}^{2-}$ = +8 J K^{-1} at 25 °C), do not affect the ice adhesion strength. This suggests that the kosmotropic ions are more effective in decreasing the ice adhesion strength than the chaotropic ones.

Another important factor that may influence the ice adhesion strength is the nature of the polyelectrolyte layer as deduced from Figure 2. For instance, it emerges on comparison of G-COO^-Li^+ and G-$SO_3^-Li^+$ that the ice adhesion strength measured on weak polyelectrolyte brush (G-COO^-Li^+) at −18 °C is very similar to bare substrate, whereas, in contrast, a significant decrease in the adhesion has been observed on strongly dissociating polyelectrolyte brush (G-$SO_3^-Li^+$). This difference between G-COO^-Li^+ and G-$SO_3^-Li^+$ can be understood in relation to XPS data which shows a sizable fraction (∼35%) of the surface carboxylate groups are converted to protonated form during the water rinsing step.

An alternative representation of the data in Figure 2 has been obtained by calculating the percentage increase/decrease in the ice adhesion strength due to various polymer brush layers. The percentage values as shown in Figure 3 was calculated by taking

dx.doi.org/10.1021/am500046d | ACS Appl. Mater. Interfaces 2014, 6, 6487−6496

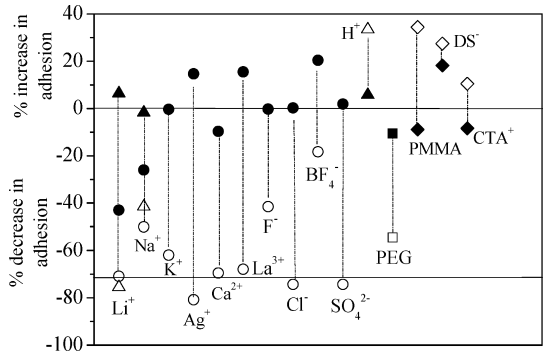

Figure 3. Percentage increase/decrease in ice adhesion strength for all the polymer brush layers. The horizontal line at zero represents the adhesion strength measured on bare glass substrate (offset from real value to zero). Filled symbols correspond to measurements at −18 °C and the open symbols correspond to measurements at −10 °C. Positive values indicate % increase in adhesion and negative values indicate % decrease in adhesion due to surface modification. Adhesion strength measured on G-$SO_3^-X^{n+}$ and G-N^+Y^{n-} (●, ○), G-COO^-Z^+ (▲, Δ), G-PEG (■, □), G-N^+DS^-, G-$SO_3^-CTA^+$ and G-PMMA (◆, ◇). The vertical dotted line connects the data points obtained at −18 °C and −10 °C for easy reading.

the difference between ice adhesion strength measured on polymer brush layers and the bare substrate at the same freezing temperature and dividing the difference by the bare glass values. The positive and negative values correspond to the percentage increase and decrease in adhesion relative to the bare substrate, respectively.

It can be seen from Figure 3 that the ice adhesion strength on polyelectrolyte brush layers with Li^+, Ag^+, Ca^{2+}, La^{3+}, Cl^-, and SO_4^{2-} counterions (G-$SO_3^-X^{n+}$ and G-N^+Y^{n-}) is significantly reduced (70−80%) at −10 °C in contrast to −18 °C. These polyelectrolyte brushes exhibit superhydrophilic behavior with very low static contact angle ($\theta_s \leq 10°$) and low hysteresis ($H < 10°$) (Table 3). In comparison with the hydrophilic brushes (G-PEG) the superhydrophilic polyelectrolyte brushes exhibits lower ice adhesion. At −18 °C, the effect of counterions on ice adhesion strength is not significant.

Overall, with the exception of poly(methacrylic acid) brush (G-COOH), the ice adhesion strength decreases with increase in freezing temperature on all hydrophilic surfaces, G-$SO_3^-X^{n+}$, G-N^+Y^{n-}, G-COO^-Z^+, and G-PEG, with static contact angle values ranging between 5 and 40°. This temperature dependency can be qualitatively explained in the context of interfacial melting of ice at the ice−substrate interface. Similar to surface-induced melting at the ice−vapor interface, measurements at the ice−silica interface using synchrotron X-ray reflection have positively identified a thin liquid-like layer (also known as a quasi liquid layer, QLL). In general, the thickness of the QLL layer increases with increase in freezing temperature although the exact temperature−thickness relationship seems to depend on the probing method.[41,45−47] It is our hypothesis that the chemical nature of polymer brush/counterions could influence the structure of QLL and thereby the propensity of water to crystallize within the brush-water interface. The exact nature of QLL on polymer brush needs to be understood at the molecular level and such studies are currently being pursued especially using surface-sensitive spectroscopic tools.

In addition to the nature of the ions, the other important factor that needs to be considered is the structure of the polyelectrolyte brushes. In the case of the strong polyelectrolyte brushes containing monovalent counterions which includes G-SO_3^- X^+ (X^+ = Li^+, Na^+ and K^+) and G-N^+Y^- (Y^- = Cl^-), the counterions dissociate fully upon contact with water. However, due to very low external ionic strength in pure water the dissociated ions are confined within the polymer brush layer. This sets up an osmotic imbalance resulting in the swelling of the polyelectrolyte brush layers. Hence the polyelectrolyte brushes comprising of monovalent counterions are in the osmotically swollen state before the commencement of freezing. We speculate that the high tendency of ions to dissociate and at the same time to stay within the brush layer may increase the thickness of the QLL at subzero temperatures.

Both experimental and theoretical studies have shown that polyelectrolyte brushes collapse significantly in the presence of multivalent counterions and thereby their thickness is reduced significantly.[48,49] Thus, multivalent ions induce significant structural reorganization of the polyelectrolyte layer and are less easily dissociated than monovalent ones. This may counteract an expansion of the QLL at subzero temperatures, explaining that polymer brushes comprising of divalent and trivalent kosmotropic ions, G-$SO_3^-Ca^{2+}$ and G-$SO_3^-La^{3+}$, exhibit high ice adhesion strength at −18 °C even though the ions interact strongly with water ($\Delta S_{struc,Ca}{}^{2+}$ = −59 J K^{-1} mol^{-1}, $\Delta S_{struc,La}{}^{3+}$ = −113 J K^{-1} mol^{-1}). It suggests that the kosmotropic ions are efficient in reducing the ice adhesion strength at low freezing temperatures only if they do not interact too strongly with polyelectrolyte brush layer.

The uncharged hydrophilic brushes, namely G-COOH (θ_s = 22°) and G-PEG (θ_s = 40°), exhibits completely opposite behaviors in terms of ice adhesion strength (Figure 3). The ice on G-COOH exhibited reproducible cohesional breakages at both freezing temperatures (see the Supporting Information, SI5) due to high adhesion strength (Figure 3). By contrast, ice on G-PEG exhibits low adhesion strength at both freezing temperatures. To better understand this difference, we investigated further on how water droplets behave under shear on G-COOH and G-PEG by measuring the advancing and receding contact angles repeatedly on the same spot. The results, as shown in Figure 4, demonstrate that the curvature of

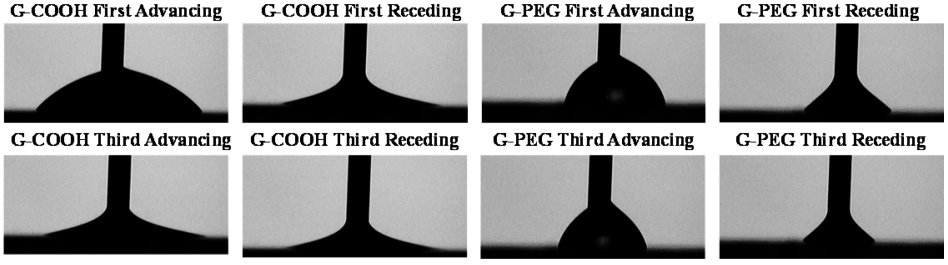

Figure 4. Consecutive measurement advancing and receding CA on G-COOH and G-PEG surfaces.

the water droplet changes from convex to concave on G-COOH during the third advancing, resulting in very low advancing contact angle (<10°). This indicates the formation of strongly bound water during the first advancement which acts as a lubricating layer during subsequent CA measurements. On the contrary, the shape of water drop and hence the advancing contact angle on G-PEG is not affected during consecutive CA measurement runs which indicates that the water molecules are not strongly bound to G-PEG. The high ice adhesion strength on G-COOH was thought to be due to the interfacial layer acting as glue between the brush and the bulk ice.

The ice adhesion strength on partially hydrophobic brush layers (θ_s = 70−90°) such as G-N^+DS^-, G-$SO_3^-CTA^+$, and G-PMMA is similar to that on the bare glass. Even though cohesional sliding was observed at −10 °C, high absolute values of ice adhesion strength indicate that the thickness of the liquid-like layer was reduced. Hence, unavailability of the free ions negatively affects the strength of ice adhesion at −10 °C. The comparison of the partially hydrophobic and super-hydrophilic coatings therefore demonstrates two principally different ice adhesion modes and implies the importance of the ion effects in the relation to the thickness of the quasi-liquid layer and measured ice adhesion strength.

In this study, we demonstrate the benefits of incorporating ions at the solid−ice interface for anti-icing applications. This study also points out the importance of ions to remain in a fully dissociated form (osmotic brush structure) for to be more effective as an anti-icing agent. As a next step we are investigating the effects of ion leaching of polyelectrolyte brushes via repeated freezing and adhesion measurement cycles under controlled environment. We are also investigating ionic sol−gel approach to release ions at a controlled rate as a coating solution. A similar approach has been used for a controlled release of anti-icing agent such as glycerol.[50] A bigger challenge that needs to be addressed in the future concerns the surface deterioration of ion based coatings when exposed to real conditions.

CONCLUSIONS

In the present work, five types of methacrylic monomers were polymerized on microscopic glass surfaces by SI-ATRP allowing for surface modification with oligo(ethylene glycol), sulfonate, quaternary ammonium and carboxylate functional groups. Coatings having ionizable groups were further used for ion exchange in order to incorporate 13 mono-, bi-, and trivalent ions (H^+, Li^+, Na^+, K^+, Ag^+, Ca^{2+}, La^{3+}, CTA^+, F^-, Cl^-, BF_4^-, SO_4^{2-}, DS^-).The strongest kosmotropes characterized by the most negative water structural entropy, Li^+ and Na^+, were able to reduce ice adhesion by 40 and 25%, respectively at −18 °C, whereas no effect on ice adhesion was observed for the weak kosmotropes and chaotropes. At −10 °C, all polyelectrolyte coatings demonstrated significant reduction in ice adhesion by 20−80%, depending on ion type. On the other hand, hydrophilic coatings composed of poly(methacrylic acid) did not reduce ice adhesion. Partially hydrophobic coatings composed of poly(methyl methacrylate) brushes or surfactant treated polyelectrolyte brushes does not reduce ice adhesion.

ASSOCIATED CONTENT

Supporting Information

A description of XPS, ellipsometry, profilometry, contact angle measurements, as well as experimental ice adhesion profiles. This material is available free of charge via the Internet at http://pubs.acs.org/

AUTHOR INFORMATION

Corresponding Author

*Tel.: +45 87155318. Fax: +45 8619 6199. E-mail: ji@eng.au.dk.

Notes

The authors declare no competing financial interest.

ACKNOWLEDGMENTS

Authors S.C. and J.I. thank Nordic Innovation for full financial support. The Nils and Dorthi Troëdsson Foundation for Scientific Research supports an adjunct professorship for A. Swerin at KTH. The work is part of Nordic research project "TopNANO", funded by industrial companies in the Nordic countries and the Top-level Research Initiative administered through Nordic Innovation.

REFERENCES

(1) Parent, O.; Ilinca, A. Anti-Icing and De-Icing Techniques for Wind Turbines: Critical Review. *Cold Reg. Sci. Technol.* **2011**, *65*, 88−96.

(2) Karmouch, R.; Ross, G. G. Experimental Study on the Evolution of Contact Angles with Temperature Near the Freezing Point. *J. Phys. Chem. C* **2010**, *114*, 4063−4066.

(3) Cao, L.; Jones, A. K.; Sikka, V. K.; Wu, J.; Gao, D. Anti-Icing Superhydrophobic Coatings. *Langmuir* **2009**, *25*, 12444−12448.

(4) Wong, T.-S.; Kang, S. H.; Tang, S. K. Y.; Smythe, E. J.; Hatton, B. D.; Grinthal, A.; Aizenberg, J. Bioinspired Self-Repairing Slippery Surfaces with Pressure-Stable Omniphobicity. *Nature* **2011**, *477*, 443−447.

(5) Menini, R.; Ghalmi, Z.; Farzaneh, M. Highly Resistant Icephobic Coatings on Aluminum Alloys. *Cold Reg. Sci. Technol.* **2011**, *65*, 65−69.

(6) Makkonen, L. Ice Adhesion —Theory, Measurements and Countermeasures. *J. Adhes. Sci. Technol.* **2012**, *26*, 413−445.

(7) Kulinich, S. A.; Farzaneh, M. How Wetting Hysteresis Influences Ice Adhesion Strength on Superhydrophobic Surfaces. *Langmuir* **2009**, *25*, 8854−8856.

(8) Kulinich, S. A.; Farzaneh, M. Ice Adhesion on Super-Hydrophobic Surfaces. *Appl. Surf. Sci.* **2009**, *255*, 8153−8157.

(9) Petrenko, V. F.; Peng, S. Reduction of Ice Adhesion to Metal by Using Self-Assembling Monolayers (SAMs). *Can. J. Phys.* **2003**, *81*, 387−393.

(10) Meuler, A. J.; Smith, J. D.; Varanasi, K. K.; Mabry, J. M.; McKinley, G. H.; Cohen, R. E. Relationships between Water Wettability and Ice Adhesion. *ACS Appl. Mater. Interfaces* **2010**, *2*, 3100−3110.

(11) Dotan, A.; Dodiuk, H.; Laforte, C.; Kenig, S. The Relationship between Water Wetting and Ice Adhesion. *J. Adhes. Sci. Technol.* **2009**, *23*, 1907−1915.

(12) Landy, M.; Freiberger, A. Studies of Ice Adhesion: I. Adhesion of Ice to Plastics. *J. Colloid Interface Sci.* **1967**, *25*, 231−244.

(13) Tourkine, P.; Le Merrer, M.; Quéré, D. Delayed Freezing on Water Repellent Materials. *Langmuir* **2009**, *25*, 7214−7216.

(14) Heydari, G.; Thormann, E.; Järn, M.; Tyrode, E.; Claesson, P. M. Hydrophobic Surfaces: Topography Effects on Wetting by Supercooled Water and Freezing Delay. *J. Phys. Chem. C* **2013**, *117*, 21752−21762.

(15) Varanasi, K. K.; Deng, T.; Smith, J. D.; Hsu, M.; Bhate, N. Frost Formation and Ice Adhesion on Superhydrophobic Surfaces. *Appl. Phys. Lett.* **2010**, *97*, 234102−3.

(16) Kulinich, S. A.; Farhadi, S.; Nose, K.; Du, X. W. Super-hydrophobic Surfaces: Are They Really Ice-Repellent? *Langmuir* **2011**, *27*, 25−29.

(17) Kim, P.; Wong, T.-S.; Alvarenga, J.; Kreder, M. J.; Adorno-Martinez, W. E.; Aizenberg, J. Liquid-Infused Nanostructured Surfaces with Extreme Anti-Ice and Anti-Frost Performance. *ACS Nano* **2012**, *6*, 6569−6577.
(18) Chen, J.; Dou, R.; Cui, D.; Zhang, Q.; Zhang, Y.; Xu, F.; Zhou, X.; Wang, J.; Song, Y.; Jiang, L. Robust Prototypical Anti-Icing Coatings with a Self-lubricating Liquid Water Layer between Ice and Substrate. *ACS Appl. Mater. Interfaces* **2013**, *5*, 4026−4030.
(19) Murase, H.; Nanishi, K. On the Relationship of Thermodynamic and Physical Properties of Polymers with Ice Adhesion. *Ann. Glaciol.* **1985**, *6*, 146−149.
(20) Murase, H.; Nanishi, K.; Kogure, H.; Fujibayashi, T.; Tamura, K.; Haruta, N. Interactions Between Heterogeneous Surfaces of Polymers and Water. *J. Appl. Polym. Sci.* **1994**, *54*, 2051−2062.
(21) Chen, J.; Liu, J.; He, M.; Li, K.; Cui, D.; Zhang, Q.; Zeng, X.; Zhang, Y.; Wang, J.; Song, Y. Superhydrophobic Surfaces Cannot Reduce Ice Adhesion. *Appl. Phys. Lett.* **2012**, *101*, 111603−3.
(22) Bascom, W. D.; Cottington, R. L.; Singleterry, C. R. Ice Adhesion to Hydrophilic and Hydrophobic Surfaces. *J. Adhes.* **1969**, *1*, 246−263.
(23) Tsarevsky, N. V.; Pintauer, T.; Matyjaszewski, K. Deactivation Efficiency and Degree of Control over Polymerization in ATRP in Protic Solvents. *Macromolecules* **2004**, *37*, 9768−9778.
(24) Tugulu, S.; Barbey, R.; Harms, M.; Fricke, M.; Volkmer, D.; Rossi, A.; Klok, H.-A. Synthesis of Poly(methacrylic acid) Brushes via Surface-Initiated Atom Transfer Radical Polymerization of Sodium Methacrylate and Their Use as Substrates for the Mineralization of Calcium Carbonate. *Macromolecules* **2006**, *40*, 168−177.
(25) Stalder, A. F.; Kulik, G.; Sage, D.; Barbieri, L.; Hoffmann, P. A Snake-Based Approach to Accurate Determination of Both Contact Points and Contact Angles. *Colloids Surf., A* **2006**, *286*, 92−103.
(26) Wang, C.; Zhang, W.; Siva, A.; Tiea, D.; Wynne, K. J. Laboratory Test for Ice Adhesion Strength Using Commercial Instrumentation. *Langmuir* **2013**, *30*, 540−547.
(27) Tsarevsky, N. V.; Braunecker, W. A.; Matyjaszewski, K. Electron Transfer Reactions Relevant to Atom Transfer Radical Polymerization. *J. Organomet. Chem.* **2007**, *692*, 3212−3222.
(28) Jones, D. M.; Brown, A. A.; Huck, W. T. S. Surface-Initiated Polymerizations in Aqueous Media: Effect of Initiator Density. *Langmuir* **2002**, *18*, 1265−1269.
(29) Huang, W.; Kim, J.-B.; Bruening, M. L.; Baker, G. L. Functionalization of Surfaces by Water-Accelerated Atom-Transfer Radical Polymerization of Hydroxyethyl Methacrylate and Subsequent Derivatization. *Macromolecules* **2002**, *35*, 1175−1179.
(30) Chernyy, S.; Iruthayaraj, J.; Ceccato, M.; Hinge, M.; Pedersen, S. U.; Daasbjerg, K. Elucidation of the Mechanism of Surface-Initiated Atom Transfer Radical Polymerization from a Diazonium-Based Initiator Layer. *J. Polym. Sci., Part A: Polym. Chem.* **2012**, *50*, 4465−4475.
(31) Dunlop, I. E.; Thomas, R. K.; Titmus, S.; Osborne, V.; Edmondson, S.; Huck, W. T. S.; Klein, J. Structure and Collapse of a Surface-Grown Strong Polyelectrolyte Brush on Sapphire. *Langmuir* **2012**, *28*, 3187−3193.
(32) Samokhina, L.; Schrinner, M.; Ballauff, M.; Drechsler, M. Binding of Oppositely Charged Surfactants to Spherical Polyelectrolyte Brushes: A Study by Cryogenic Transmission Electron Microscopy. *Langmuir* **2007**, *23*, 3615−3619.
(33) Konradi, R.; Rühe, J. Binding of Oppositely Charged Surfactants to Poly(methacrylic acid) Brushes. *Macromolecules* **2005**, *38*, 6140−6151.
(34) Combellas, C.; Kanoufi, F.; Sanjuan, S.; Slim, C.; Tran, Y. Electrochemical and Spectroscopic Investigation of Counterions Exchange in Polyelectrolyte Brushes. *Langmuir* **2009**, *25*, 5360−5370.
(35) Yang, X.-F.; Ye, S.-J.; Bai, Q.; Wang, X.-Q. A Fluorescein-Based Fluorogenic Probe for Fluoride Ion Based on the Fluoride-Induced Cleavage of Tert-butyldimethylsilyl Ether. *J. Fluoresc.* **2007**, *17*, 81−87.
(36) Osborne, V. L.; Jones, D. M.; Huck, W. T. S. Controlled Growth of Triblock Polyelectrolyte Brushes. *Chem. Commun.* **2002**, 1838−1839.
(37) Côté, A. P.; Shimizu, G. K. H. Silver(I) Arylsulfonates: A Systematic Study of "Softer" Hybrid Inorganic−Organic Solids. *Inorg. Chem.* **2004**, *43*, 6663−6673.
(38) Li, F.-F.; Ma, J.-F.; Yang, J.; Liu, Y.-Y. Synthesis and Crystal Structure of a Novel Silver Sulfonate Involving Ag−C Interactions. *J. Chem. Crystallogr.* **2008**, *38*, 525−528.
(39) Moglianetti, M.; Webster, J. R. P.; Edmondson, S.; Armes, S. P.; Titmuss, S. A Neutron Reflectivity Study of Surfactant Self-Assembly in Weak Polyelectrolyte Brushes at the Sapphire−Water Interface. *Langmuir* **2011**, *27*, 4489−4496.
(40) Ishikubo, A.; Mays, J.; Tirrell, M. Behavior of Cationic Surfactants in Poly(styrene sulfonate) Brushes. *Ind. Eng. Chem. Res.* **2008**, *47*, 6426−6433.
(41) Jellinek, H. H. G. Liquid-Like (Transition) Layer on Ice. *J. Colloid Interface Sci.* **1967**, *25*, 192−205.
(42) Wang, H.; Tang, L.; Wu, X.; Dai, W.; Qiu, Y. Fabrication and Anti-Frosting Performance of Super Hydrophobic Coating Based on Modified Nano-Sized Calcium Carbonate and Ordinary Polyacrylate. *Appl. Surf. Sci.* **2007**, *253*, 8818−8824.
(43) Marcus, Y. Effect of Ions on the Structure of Water: Structure Making and Breaking. *Chem. Rev.* **2009**, *109*, 1346−1370.
(44) Marcus, Y. Viscosity *B*-coefficients, Structural Entropies and Heat Capacities, and the Effects of Ions on the Structure of Water. *J. Solution Chem.* **1994**, *23*, 831−848.
(45) Fletcher, N. H. Surface Structure of Water and Ice. *Philos. Mag.* **1962**, *7*, 255−269.
(46) Petrenko, V. F. Study of the Surface of Ice, Ice/Solid and Ice/Liquid Interfaces with Scanning Force Microscopy. *J. Phys. Chem. B* **1997**, *101*, 6276−6281.
(47) Engemann, S.; Reichert, H.; Dosch, H.; Bilgram, J.; Honkimäki, V.; Snigirev, A. Interfacial Melting of Ice in Contact with SiO_2. *Phys. Rev. Lett.* **2004**, *92*, 205701.
(48) Guo, X.; Ballauff, M. Spherical Polyelectrolyte Brushes: Comparison Between Annealed and Quenched Brushes. *Phys. Rev. E* **2001**, *64*, 051406.
(49) Jiang, T.; Wu, J. Ionic Effects in Collapse of Polyelectrolyte Brushes. *J. Phys. Chem. B* **2008**, *112*, 7713−7720.
(50) Ayres, J.; Simendinger, W. H.; Balik, C. M. Characterization of Titanium Alkoxide Sol−Gel Systems Designed for Anti-Icing Coatings: I. Chemistry. *J. Coat. Technol. Res.* **2007**, *4*, 463−471.